IBRACON Structures and Materials Journal
Revista IBRACON de Estruturas e Materiais
ISSN 1983-4195 ismj.org

ORIGINAL ARTICLE

Structural analysis of RC infilled frames with participating masonry: a proposal procedure for multi-strut models

Análise estrutural de pórticos de concreto armado preenchidos com alvenarias participantes: proposta de procedimento para o uso de modelos de múltiplas diagonais

Lucas Ferreira Galvão[a]
Gerson Moacyr Sisniegas Alva[a]

[a]Universidade Federal de Uberlândia – UFU, Faculdade de Engenharia Civil, Uberlândia, MG, Brasil

Received 24 July 2022
Accepted 02 November 2022

Abstract: In this paper, a procedure is proposed for the use of multi-strut models for the structural analysis of RC frames infilled with participating masonry subjected to lateral loads. It is therefore proposed that the eccentricities of the equivalent struts be obtained from the equivalent strut width of the classic single-strut model, whose value can be estimated from analytical expressions in the literature. The proposed models are validated by Finite Element Method (FEM) modeling, which simulates the contact between the infill masonry and the frame. It could be concluded that the proposed modeling provided better results than the classic single-strut model in obtaining the maximum shear force acting in the columns. It was also noted that the differences of the equivalent strut models in relation to the FEM results were higher with the increase of the participating masonry stiffness.

Keywords: infilled frames, participating masonry, equivalent strut models, RC structures, structural analysis.

Resumo: Neste trabalho é proposto um procedimento para o uso de modelos de diagonais equivalentes múltiplas na análise estrutural de pórticos de concreto armado preenchidos com alvenarias participantes submetidos a carregamentos horizontais. Propõe-se que as excentricidades das diagonais equivalentes sejam obtidas a partir da largura da diagonal equivalente do modelo clássico de diagonal única, cujo valor pode ser obtido a partir de expressões analíticas da literatura. Os modelos propostos são validados por meio de modelagem via Método dos Elementos Finitos (MEF) que simula o contato alvenaria-pórtico. Concluiu-se que a modelagem proposta forneceu resultados melhores que o modelo clássico de diagonal única na obtenção da máxima força cortante atuante nos pilares. Notou-se também que as diferenças dos modelos de diagonais equivalentes em relação aos resultados MEF foram maiores com o aumento da rigidez da alvenaria participante.

Palavras-chave: pórticos preenchidos, alvenarias participantes, modelos de diagonal equivalente, estruturas de concreto armado, análise estrutural.

How to cite: L. F. Galvão and G. M. S. Alva, “Structural analysis of RC infilled frames with participating masonry: a proposal procedure for multi-strut models”, *Rev. IBRACON Estrut. Mater.*, vol. 16, no. 4, e16409, 2023, https://doi.org/10.1590/S1983-41952023000400009

1 INTRODUCTION

The recognized influence of masonry infill walls on the static and dynamic behavior of framed structural systems, subjected to lateral loads, is documented in international research, and has been investigated in Brazil in the last two decades (studies are cited in section 2 of this paper). However, the masonry infill walls with a structural role on the framed building structures has still not been consolidated into Brazilian structural design offices.

Corresponding author: Gerson Moacyr Sisniegas Alva. E-mail: alva_gerson@yahoo.com.br
Financial support: CNPq (Process: 308720/2018-0).
Conflict of interest: Nothing to declare.
Data Availability: The data that support the findings of this study are available from the corresponding author, GMSA, upon reasonable request.

The masonry infill walls with a structural role are denominated as *participating masonry.* According to the definition of the recently updated Standard Brazilian code of structural masonry – ABNT NBR 16868-1 [1] – the participating masonry is the structural masonry built within a frame, which is intentionally designed and built as part of the bracing system.

In annex D of ABNT NBR 16868-1 [1], the equivalent strut model is recommended for simulating the contribution of participating masonry on frame stiffness, observing that the elements of the frame should be designed for the additional shear forces introduced by diagonal strut action, due to the contact of the wall with the beams and the columns. However, the code does not present an equivalent strut model that is specific to such a consideration. Since the classic single-strut models are not capable of capturing additional shear forces produced on the contact between masonry wall and frame, the use of two-strut and three-strut models becomes more appropriate for this purpose.

The main objective of this paper is to present a proposal for the definition of the eccentricities of diagonal struts in multiple equivalent strut models (specifically two-struts and three-struts models). It is proposed that these eccentricities be calculated as a function of the equivalent strut width, which can be obtained from the expressions available in specialized literature. Numerical simulations of RC frames infilled with participating masonry were conducted to evaluate the maximum shear force acting on the column, using Finite Element Method (reference model, which simulates the infill wall-frame contact problem) and using the proposed procedure for multi-strut models. Additionally, an analysis is made concerning the influence of the equivalent strut width expression used in the simulations and the influence of the stiffness of the masonry in the quality of the results provided by the proposed procedure. It is also noteworthy that the masonry was considered as a material with orthotropic behavior in the analyzes conducted.

2 PREVIOUS RESEARCH

In international specialized literature, several experimental and numerical studies on the behavior of masonry infilled frames subjected to lateral loads are found, where most of such studies are dedicated to seismic loads. In Brazil, even with the number of studies being small regarding international research, the theme has more recently gained prominence, especially over the last two decades. From these national studies, the following can be cited: Alvarenga [2], Santos [3], Silva [4], Sousa [5], Alva et al. [6], Pitanga [7], Montandon [8], Grandi [9], Medeiros [10], Santos [11], Queiroz [12], Rigão [13] and Galvão [14].

Following the growing development of the theme in Brazil, it can be quoted the addition of an informative annex (annex D) in the recent update to the Brazilian code of structural masonry – ABNT NBR 16868-1 [1] –, which addresses the consideration of participating masonry.

Among the pioneering authors in the study of infilled frames, Polyakov [15] should be mentioned, who after conducting a series of experiments and describing the behavior of the infill-frame ensemble, when submitted to lateral loads, proposes an analytical technique in which the masonry infilled frame system is equivalent to a frame where the masonry is substituted by an equivalent diagonal strut. This structural model is denominated as the Equivalent Strut Model (ESM).

The originally proposed ESM consists in simulating the masonry wall by a pin-jointed diagonal strut, defined on the beam-column connection points of the frame. In this way, this model can be denominated as classic ESM. Based on the classic ESM, other analytical models have been proposed in the literature, including those with multiple struts simulating the behavior of masonry.

To apply the classic ESM, it is necessary to define the mechanical and geometric properties of the equivalent strut. Models proposed by Polyakov [15], Holmes [16], Stafford-Smith [17]–[20], Stafford-Smith and Carter [21] and Hendry [22] use different parameters for the equivalent strut, but all of them are dependent on the dimensions and mechanical properties of the infill masonry and the frame members.

One of the key parameters on the classic ESM is the width of the equivalent strut, which can be calculated by analytical expressions proposed by different authors, as: Mainstone [23], Liauw and Kwan [24], Decanini and Fantin [25], Paulay and Priestley [26], Durrani and Luo [27], Chrysostomou and Asteris [28] and Montandon [8].

Despite the existence of various expressions for calculating the width of the equivalent strut, their results tend to differ one from the other. Thus, the choice of the most adequate expression for the equivalent strut width is a difficult task. In their respective studies, Montandon [8] and Queiroz [12] confirm these differences, with variations of up to 212% in the values obtained for the width of the equivalent strut.

Still regarding the classic ESM, it is noteworthy that due to its ease application, such model has become the most studied and widespread in technical community. This model is also recommended by different codes, including American codes FEMA 306 [29] and TMS 402/602 [30], Canadian code CSA S304 [31], New Zealand code NZS 4230 [32], and the Brazilian code ABNT NBR 16868-1 [1].

However, although it is the best known and most used for considering the contribution of masonry walls in infilled frames, the classic ESM does not provide satisfactory results concerning the local effects on the frame members, mainly when it comes to internal shear forces and the bending moment acting on columns and beams. Statements confirming the can be found in studies by El-Dakhakhni et al. [33], Crisafulli and Carr [34], Yekrangnia and Mohammadi [35], Rigão [13] and Galvão [14]. From such assumption, these authors proposed analytical models with modifications regarding the classic ESM, on which the masonry wall is simulated by equivalent multiple struts.

To illustrate that the classic single-strut ESM is inadequate for capturing the maximum shear force in the column (that occurs in the contact region with the infill masonry), some results obtained by Galvão [14] are represented in Figure 1. The author analyzed RC frames, infilled with participating masonry, subjected to a monotonic lateral load. Masonries with different modulus of elasticity were analyzed, and in Figure 1 are shown the results for three cases, containing the shear force diagram for the column of the frame, which are obtained by classic single-strut models and by a Finite Element Method (FEM) model, used as a reference. It should be noted that were used the expressions from Mainstone [23], Durrani and Luo [27] and ABNT NBR 16868-1 [1] for the calculation of the equivalent strut width, which are represented, respectively, as MA, DL and NBR in Figure 1.

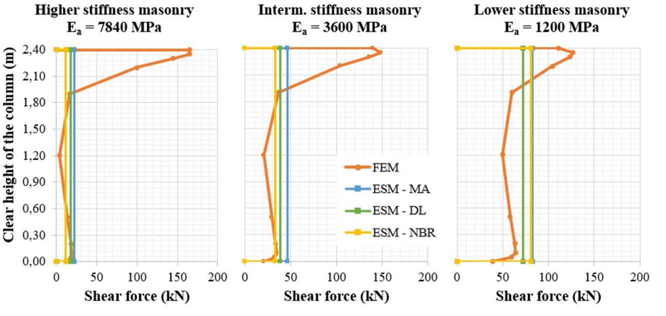

Figure 1. Shear force diagram along the clear height of the column (FEM x Classic single-strut ESM) – Galvão [14].

From Figure 1, it can be noticed that the classic model does not provide satisfactory results for the maximum shear force acting in the column, which occurs at the contact region with the infill wall. The stiffer the infill masonry, the more inaccurate are the results provided by the classic model.

3 PROPOSED PROCEDURE FOR MULTIPLE STRUT MODEL

With the aim of obtaining analytical models that predict in an efficient and precise manner the behavior of infilled frames with participating masonry subjected to lateral loads, and which have a simple and practical application, a procedure for the elaboration of ESM models with two and three struts was proposed for considering the contribution of the participating masonry.

Different to the classic ESM, in which the single diagonal strut is defined on the intersection between the beam and column nodes, the models with multiple struts present eccentric struts, which are defined through a given eccentricity from the beam-column joint. Crisafulli and Carr [34] emphasize that these eccentricities affect the lateral stiffness of the structure and are important parameters to be obtained.

The procedure proposed in this study was elaborated based on ESM preliminary models analyzed by Crisafulli and Carr [34], represented in Figure 2. In these models, the sum of the areas of the cross sections of the equivalent struts was considered as equal for all situations, adopting, in this sense, the following considerations: on two-strut ESM, both have the same area of cross section, equivalent to half of the area of the strut on the classic ESM; on the three-strut ESM, the area of the cross section of the central strut was adopted as being twice that of the eccentric struts, as illustrated in Figure 2c. In regard to the position of the eccentric struts, the authors consider the values of the eccentricities as equal to fractions of the contact length (α_H) estimated by the expressions of Stafford-Smith and Carter [21] and Hendry [22].

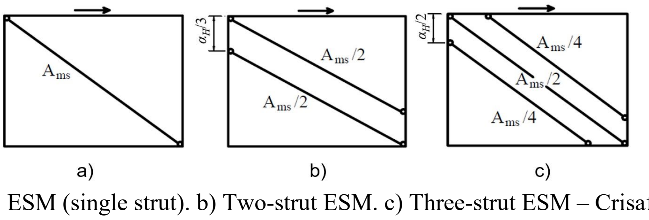

Figure 2. a) Classic ESM (single strut). b) Two-strut ESM. c) Three-strut ESM – Crisafulli and Carr [34].

For the model proposed in the present study, the distribution of struts and the consideration of their cross-sectional areas were adopted as being equal to those indicated in the preliminary models of Crisafulli and Carr [34]. However, the eccentricities were obtained by a different procedure, which was based on conclusions obtained by Montandon [8] and Di Nino [36]. These authors pointed out that the contact lengths given by the expressions of Stafford-Smith and Carter [21] and Hendry [22] were significantly higher than those observed in their reference models simulated via FEM.

Thus, aiming to achieve appropriate eccentricities for the equivalents struts, the procedure proposed in this paper is that the eccentricities of the diagonal struts be calculated as a function of the width of the equivalent strut (w), which in turn can be calculated by different expressions and procedures available in the literature and in normative codes.

In Figure 3 is shown a general infilled framed and its equivalent strut, where w is the equivalent strut width and θ is the angle between the equivalent strut and the horizontal axis. From these two parameters, the proposal procedure consists in obtaining the effective contact lengths between column and infill wall ($\alpha_{ef,H}$) and between beam and infill wall ($\alpha_{ef,L}$) through geometric calculations. Once these geometries are defined, the eccentricities e_H and e_L are obtained through geometry, being also dependent on the dimensions of the cross sections of the column (h_p) and of the beam (h_v) on the plane of the infilled frame.

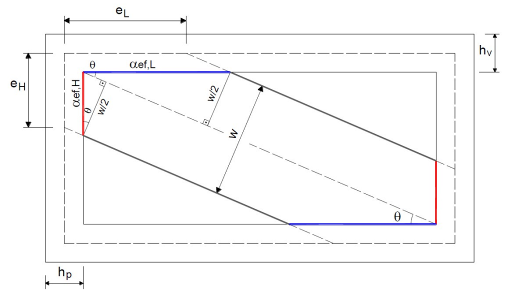

Figure 3. Parameters for the application of the proposed models

Thus, the expressions for the calculations of the parameters $\alpha_{ef,H}$, $\alpha_{ef,L}$, e_H and e_L are presented in Equations 1 to 4.

$$\alpha_{ef,H} = \frac{w}{2 \cdot \cos\theta} \tag{1}$$

$$\alpha_{ef,L} = \frac{w}{2 \cdot \text{sen}\,\theta} \; or \; \frac{\alpha_{ef,H}}{\tan\theta} \tag{2}$$

$$e_H = \frac{h_v}{2} + \alpha_{ef,H} - \frac{h_p}{2} \cdot \tan\theta \tag{3}$$

$$e_L = \frac{h_p}{2} + \alpha_{ef,L} - \frac{h_v}{2 \cdot \tan\theta} \tag{4}$$

With the definition of the eccentricities, the positioning of the equivalent struts on the models of two and three struts are represented in Figures 4a and 4b, respectively.

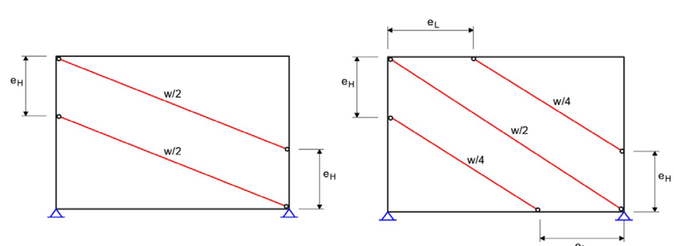

a) b)

Figure 4. a) Model with two equivalent struts. b) Model with three equivalent struts.

4 NUMERICAL SIMULATIONS

To evaluate the behavior of the proposed procedure for ESM models with two or three struts, numerical simulations were performed on frames infilled with participating masonry, for different geometric and mechanical properties. The results obtained from these simulations were compared to the results obtained through the employment of the Finite Elements Methods (FEM) and with the classic ESM. As the FEM has a more refined analysis (higher hierarchy), the results obtained from such models were considered as a reference for the analyses.

The FEM models were developed on the computer program ANSYS, Mechanical platform APDL version 2021 R1. For the ESM models, the plane frame structural analysis program FTOOL was employed.

4.1 General parameters

Numerical models were developed for single-story, single-bay participating masonry RC infilled frame without openings. The models were subjected only to a monotonic lateral load. The static scheme is illustrated in Figure 5. Highlighted here is that linear elastic analyses were performed for all models.

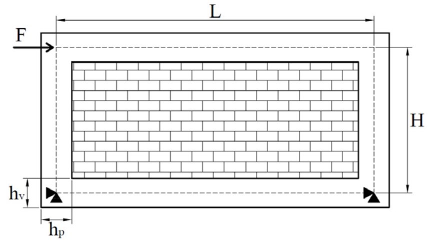

Figure 5. Static scheme of the infilled frame models

The members of the frame are composed of reinforced concrete, which was assumed linear-elastic isotropic material as a simplification. For the participating masonry, it was assumed ungrouted hollow concrete/clay structural blocks, with different values for the characteristic axial compressive strength (f_{bk}). The mechanical properties of the masonry, values of compressive strength of the mortar (f_a) and the prism (f_{pk}), as well as the minimum face shell thickness of the block, were all estimated by means of specifications suggested by ABNT NBR 16868-1 [1], which is a function of the material and strength of the block adopted for each model. On the other hand, the infill masonry was assumed as linear elastic orthotropic material.

4.2 FEM modeling

In accordance with the classification proposed by Lourenço [37], a macro-modeling was used for the numerical simulation of the behavior of the participating masonry, i.e., without distinction between blocks and mortar, treating the masonry as a continuous and homogenous element. This a more practical approach, due to the reduction in time and of computational requirements for processing the models.

The finite element PLANE182 was chosen for the modeling of the concrete frame and the infill wall. This finite element is applicable to the plane stress state and is defined by four nodes, with two degrees of freedom at each node, which are the translations in the x and y directions. These directions define the xy plane, where is located the infilled frame. Based on a mesh refinement study, finite elements of 5 cm x 5 cm were employed for the frame, as well as for the masonry. The convergence study included the analysis of stabilization of penetrations and contact pressures among the frame-masonry surfaces. Figure 6 represents one of the infilled frame models simulated on FEM.

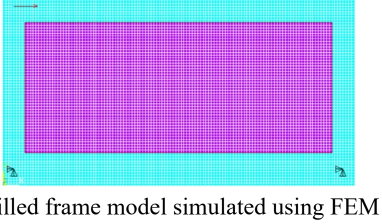

Figure 6. Infilled frame model simulated using FEM (ANSYS).

For the analysis of infilled frames using FEM, contact modeling between the elements of the frame and the masonry is necessary, to allow for sliding and separation between contact surfaces. This modeling is described in section 4.2.1.

4.2.1 Contact modeling at frame-infill wall interface

The consideration of the contact between the infill wall and the frame is of extreme importance in the modeling of infilled frames, since when subjected to lateral loads, there is a stress concentration on the compression corners of the infill wall and separation of the elements in the opposite corners. This behavior is represented in Figure 7a, obtained from the simulation of one of the models analyzed in this study. In Figure 7b are the principal compressive stresses acting in the masonry wall for the same model are illustrated, where it can be noticed the expected formation of diagonal compression in the masonry.

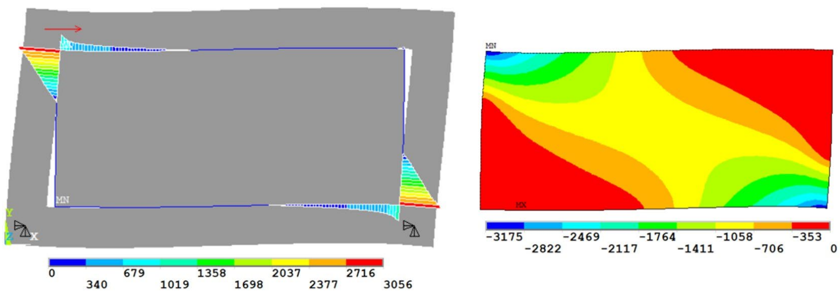

a) b)

Figure 7. a) Deformed shape of the infilled frame and contact pressure between frame and wall (kPa). b) Principal compressive stresses in the masonry (kPa).

Figure 7a shows the contact pressure that acts on the frame members. This contact pressure causes an addition of shear forces on the columns and beams of the frame. This behavior is one of the focuses of this study for using of multiple strut models.

To simulate slippage and the separation between surfaces (contact problem), elements CONTA172/TARGE169 were employed.

Ideally, there should be no penetration between the surfaces of the RC frame and the infill masonry wall. However, the numerical techniques usually applied in the solution of the contact problem may imply the existence of a small penetration. On the ANSYS computer program, two coefficients were used for controlling penetration: FKN (normal stiffness factor) and FTOLN (penetration tolerance factor). The methodology employed for choosing from these coefficients were the same as those used by Montandon [8] and Queiroz [12], which were substantiated in the study by Silva [38]. The FKN factor was calibrated for each model in order that the lowest penetration possible be obtained between the surfaces, without causing numerical inconsistencies (convergence problems); the FTOLN factor was maintained using the value standardized by ANSYS, equal to 0.1.

Other parameters to be defined in the contact problem are the friction coefficient between the frame-masonry surfaces (μ), the maximum shear strength (stress) between the surfaces ($f_{v,max}$) and cohesion (τ_0). The friction coefficient (μ) and cohesion (τ_0) were obtained from ABNT NBR 16868-1 [1] recommendations, which are a function of the average compressive strength of the mortar (f_a), that can be defined as a function compressive strength of the unit (f_{bk}).

However, the maximum shear strength (stress) ($f_{v,max}$) was determined by Equation 5 (where θ is the inclination angle of the strut with respect to the horizontal), obtained by assuming that $f_{v,max}$ cannot be higher than the shear strength of the masonry wall. Highlighted here is that, in the deduction of Equation 5, the vertical component of the compression strut force was considered, while the vertical compression stress due to masonry self-weight was disregarded.

$$f_{v,max} = \frac{\tau_0}{1-\mu \cdot tan\theta} \tag{5}$$

4.2.2 Obtaining shear force in the columns

The shear forces acting on the columns were obtained by numerical integration of the shear stresses along the cross section of these members, which were provided by program ANSYS. This process is presented in more details by Galvão [14].

4.3 FEM model validation

The accuracy of the FEM modeling procedure was made with experimental results available in the literature. Van and Lau [39] conducted an experimental study on half-scale, single-story, single-bay RC frames with unreinforced masonry infills under monotonic and cyclic loadings. As only monotonic loads were applied in the present paper, only the experimental specimens with this characteristic were analyzed for the validation of the FEM model (specimens BF1, IF1 and IF3 of Van and Lau's [39] study).

In Figure 8a is illustrated the geometry and reinforcing details of RC frames of the specimens, while in Figure 8b the lateral load-drift ratio responses of test specimens subjected to lateral monotonic loading is represented.

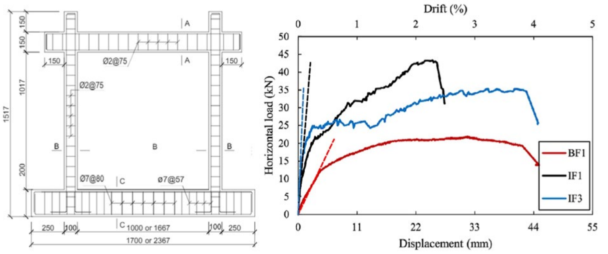

a) b)

Figure 8. a) Geometry and reinforcing details of RC frames (dimensions in mm). b) Lateral load-drift ratio responses of test specimens subjected to lateral monotonic loading – Van and Lau [39].

As only linear elastic analyzes were performed in the present paper, the initial stiffness of the experimental specimens (determined from the load and the displacement at starting of crack) were compared with the FEM models outcome. The results are disposed in the Table 1 and illustrated in Figure 8b (the dashed lines represent the initial stiffness obtained in FEM models).

Table 1. Load of first crack, displacement and initial stiffness of experimental specimens and FEM models.

Specimen	Load at starting of crack (kN)	Van and Lau [39]		FEM models	
		Displacement (mm)	Init. stiffness (kN/mm)	Displacement (mm)	Init. stiffness (kN/mm)
BF1	11.38	3.74	3.04	3.64	3.12 (+ 3%)
IF1	9.42	0.55	17.13	0.51	18.56 (+ 8%)
IF3	11.38	0.48	23.71	0.50	22.77 (- 4%)

Analyzing the results, low differences were observed between the initial stiffness obtained experimentally and numerically (FEM), indicating that the modeling used in this paper provides satisfactory results for linear elastic analyzes of RC frames infilled with masonry.

4.4 ESM modeling

Classic ESM models (single equivalent strut defined on the beam-column joint) and ESM models with two or three equivalent struts were simulated, in accordance with the procedures proposed in section 3.

Based on studies by Montandon [8] and Queiroz [12], the choice was made for using the expressions from Mainstone [23] and Durrani and Luo [27] for the equivalent strut width, since those ones present better results when compared to results via FEM modeling. The expressions used for calculating the equivalent strut width (w) are shown on Table 2 (including ABNT NBR 16868-1 [1]). The parameters used by the expressions are illustrated in Figure 9.

Highlighted here is that for the recommended expression by ABNT NBR 16868-1 [1], the equivalent strut width is the effective width (w_{eff}) and the masonry thickness is t_{ap} (described below).

Table 2. Analytical equations for calculation of the equivalent strut width.

Authors	Expression
Mainstone [23]	$w = 0.175 \cdot (\lambda_H)^{-0.4} \cdot D$
	$\lambda_H = H \cdot \sqrt[4]{\frac{E_a \cdot t \cdot sen(2\theta)}{4 \cdot E_p \cdot I_p \cdot h}}$
Durrani and Luo [27]	$w = \gamma \cdot sen(2\theta) \cdot D$
	$\gamma = 0.32 \cdot \sqrt{sen(2\theta)} \left(\frac{H^4 \cdot E_a \cdot t}{m \cdot E_p \cdot I_p \cdot h}\right)^{-0.1}$
	$m = 6 \cdot \left(\frac{1 + 6 \cdot E_v \cdot I_v \cdot H}{\pi \cdot E_p \cdot I_p \cdot L}\right)$
ABNT NBR 16868-1 [1]	$w_{eff} = \frac{\sqrt{\alpha_H^2 + \alpha_L^2}}{2} \leq \frac{D}{4}$
	$\alpha_H = \frac{\pi}{2} \cdot \sqrt[4]{\frac{4 \cdot E_p \cdot I_p \cdot h}{E_a \cdot t_{ap} \cdot sen(2\theta)}}$
	$\alpha_L = \pi \cdot \sqrt[4]{\frac{4 \cdot E_v \cdot I_v \cdot l}{E_a \cdot t_{ap} \cdot sen(2\theta)}}$

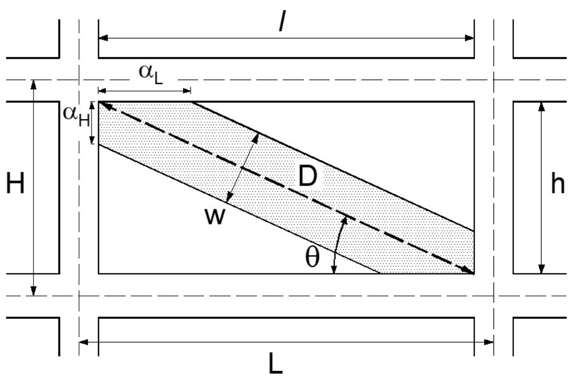

Figure 9. Parameters for the calculation of the equivalent strut width – Silva [4].

where:
D – diagonal length of the masonry infill wall;
E_a – modulus of elasticity of the masonry infill wall;
E_p – modulus of elasticity of the column;
E_v – modulus of elasticity of the beam;
H – height between beam axes (floor-to-floor distance)
h – height of masonry infill wall;
I_p – second moment of area of the column;
I_v – second moment of area of the beam;
L – distance between column axes;
l – length of the masonry infill wall;
t – wall thickness;
t_{ap} – equals two times the sum of the face shells thickness for hollow block units or the thickness of the wall for solid or fully grouted hollow block units;
w – equivalent strut width;

w_{eff} – effective equivalent strut width;

α_H –column-infill wall contact length;

α_L – beam-infill wall contact length;

θ – angle of diagonal strut measured from the horizontal;

λ_H – dimensionless relative stiffness parameter.

The static scheme adopted for the classic ESM model is represented in Figure 10. For those models with two or three struts, the scheme is analogous.

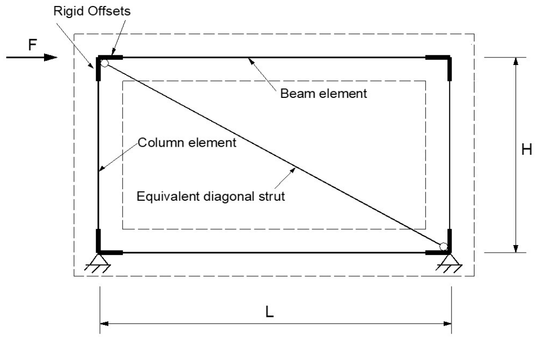

Figure 10. Infilled frame static scheme simulated by classic ESM – Alva et al. [6].

4.4.1 Analysis of the effective stiffness of the equivalent strut

For the ESM models, where the recommendations of ABNT NBR 16868-1 [1] are adopted, it was necessary to perform an additional procedure for the analysis of the effective stiffness of the equivalent strut. The Brazilian code indicates that the effective stiffness of the equivalent strut (K_{eff}) used in the calculations of the internal forces and displacements is defined according to Equation 6.

$$K_{eff} = \frac{\varphi_{st} \cdot w_{eff} \cdot t_{ap} \cdot E_a}{l_s} \tag{6}$$

where φ_{st} is the factor to account stiffness reduction in the equivalent strut (equal to 0.5) for the analysis of wall cracking (not applied in this study, since only linear elastic analyses were performed) and l_s is the design length of the equivalent strut, obtained through the subtraction of the diagonal length (D) by its effective width (w_{eff}).

Based on mechanical problems of frames members, the axial stiffness of a member is represented by EA/L, where A is the area of the cross section, E is the modulus of elasticity and L is the theoretical length of this element (calculated from the coordinates of the start node and end node of the element). In the case of the equivalent strut, the theoretical length considered by the program is obtained from the origin of the axes of the frame elements. However, the length l_s is lower than the theoretical length of the equivalent strut. As such, it is necessary to adjust the axial stiffness of this strut in programs for plane frames analysis. The proposal is made in this study that this adjustment be performed by means of the inclusion of a coefficient β according to Equation 7:

$$\beta = \frac{\sqrt{H^2+L^2}}{\sqrt{h^2+l^2} - w_{eff}} \tag{7}$$

Highlighted here is that Equation 7 was applied only to the classic ESM models (with a single strut), calculated using the recommendations from ABNT NBR 16868-1 [1]. For models with two and three equivalent struts, the expression undergoes some changes, being obtained in an analogous manner to that presented above.

4.5 Analysis of orthotropic masonry

Masonry is a material that presents a complex behavior, due to its anisotropic and heterogeneous properties, which difficult the definition of the parameters that should be adopted in the numerical models. It is for this reason that on many occasions it becomes convenient to use masonry as a material with an isotropic behavior in numerical simulations, with the aim of simplifying the model, since it reduces the number of material parameters. Such simplifications were employed by Montandon [8] and Queiroz [12], based on the conclusions by Doudoumis [40].

However, studies such as those from El-Dakhakhni et al. [33] and Cavaleri et al. [41] investigated masonry as an orthotropic material, in a way to approximate the anisotropic behavior in numerical simulations. El-Dakhakhni et al. [33] suggested adopting the modulus of elasticity parallel to bed joints (E_x) at a value of 70% the modulus of elasticity parallel to the head joints (E_y), which in turn is equivalent to the elasticity modulus normally employed in analyses that consider masonry as an isotopic material (E_a).

Cavaleri et al. [41] proposed an expression for calculating the modulus of elasticity of the infill masonry along the diagonal direction (E_d), which was obtained by means of experiments performed with distinct types of masonry. In addition, to obtain the expression, the authors consider masonry as an orthotropic material. As such, the modulus of elasticity E_d is obtained by means of Equation 8, where it is dependent on the modulus E_x and E_y, on the inclination angle of the diagonal (θ), as well as on the shear modulus of elasticity (G) and Poisson's coefficient (v), both related to the xy plane.

$$\frac{1}{E_d} = \frac{1}{E_x} \cdot (\cos\theta)^4 + \left[\frac{1}{G} - \frac{2v}{E_x}\right] \cdot (\text{sen}\,\theta \cdot \cos\theta) + \frac{1}{E_y} \cdot (\text{sen}\,\theta)^4 \tag{8}$$

In Figure 11, the scheme that considers the modulus of elasticity of the masonry in the diagonal direction is represented.

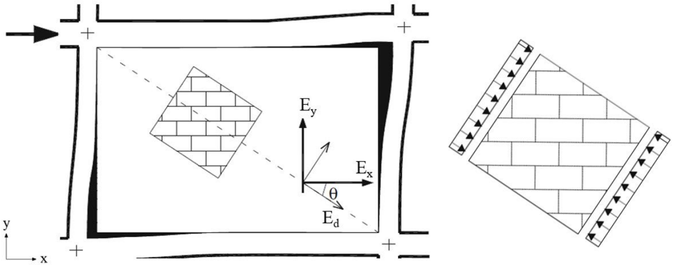

Figure 11. Scheme for considering the modulus E_d – Cavaleri et al. [41].

The simulation of the FEM models in this study took into consideration the recommendation of El-Dakhakhni et al. [33], when considering masonry as orthotropic material (E_x = 0,7 · E_y). However, for the ESM models, the E_d modulus was employed, which was calculated by Equation 8, as proposed in Cavaleri et al. [41], with the recommendation of El-Dakhakhni et al. [33] for the obtainment of the modulus E_x and E_y.

4.6 The analyzed models

Twenty-four different models of RC frames infilled with participating masonry subjected to monotonic lateral loads were simulated, following the static scheme already illustrated in Figure 6. The properties of the infilled frames to be analyzed were chosen to simulate the structural condition of a frame belonging to a tall building subjected to lateral wind loads. The masonry was considered as material with orthotropic behavior for all the models and the analyses were linear elastic. For all the models, the following properties were considered:

- Span of the beam (distance between column axes) (L) = 6.0 m;
- Floor-to-floor distance (H) = 3.0 m;
- Wall thickness (t) = 19 cm;
- Modulus of elasticity of reinforced concrete (E_c) = 35 GPa;
- Cross section of beams (b_v x h_v) = 19 cm x 60 cm.

The parameters varied between the models were: the dimensions of the cross sections of the RC columns, the structural block of the participating masonry and the lateral load applied (*F*). The cross-section heights analyzed for the column (h_p) were 60, 80, 100 and 120 cm, while its width (b_p) was considered the same in all models, equals to 19 cm.

Regarding the masonry, six distinct types of structural blocks were considered, arranged in Table 3, where the prefix were used to name the numerical models.

Table 3. Structural blocks analysed.

Prefix	Structural Block Type	f_{bk} (MPa)	E_a (MPa)
BVC04	Hollow concrete block	4.0	2560
BVC14	Hollow concrete block	14.0	7840
BVC24	Hollow concrete block	24.0	10800
BCPV04	Clay block with hollow walls	4.0	1200
BCPM10	Clay block with solid walls	10.0	3600
BCPM18	Clay block with solid walls	18.0	6480

4.6.1 Determination of the lateral load applied in each model

To determine the value of the lateral load (*F*) applied on each model, it was considered the model proposed by Liberatore and Decanini [42] to estimate the maximum strength of the infill masonry. This model was studied by Noh et al. [43].

Firstly, for each model analyzed in this paper, were calculated the corresponding failure stresses for four masonry failure modes: (a) diagonal tension; (b) sliding shear; (c) corner crushing; and (d) diagonal compression. Then, if the infill strength corresponds to the minimum value among the four-failure modes, the strength of the equivalent strut was obtained. The lateral load to be applied to the infilled frame that causes in the equivalent strut (whose properties were estimated by the procedure proposed by Liberatore and Decanini [42]) a diagonal force with the same magnitude as the infill strength previously obtained. This lateral load (*F*) was calculated and applied in each one of the numeric models of this paper, which values are shown in Table 4.

It is important to highlight that the analyzes performed were linear elastic. In a real design application, it is necessary to consider the non-linear effects, even in a simplified way (e.g., linear analysis with global stiffness reductions applied in the structural elements, which is recommended by several structural design codes).

Table 4. Lateral load (*F*) applied in each numeric model.

Model	F (kN)	Model	F (kN)
BVC04P60	166	BVC04P100	154
BVC14P60	345	BVC14P100	319
BVC24P60	337	BVC24P100	312
BCPV04P60	191	BCPV04P100	177
BCPM10P60	372	BCPM10P100	344
BCPM18P60	350	BCPM18P100	324
BVC04P80	160	BVC04P120	149
BVC14P80	331	BVC14P120	308
BVC24P80	324	BVC24P120	301
BCPV04P80	184	BCPV04P120	171
BCPM10P80	357	BCPM10P120	332
BCPM18P80	336	BCPM18P120	312

4.6.2 Remaining parameters

The remaining parameters of the numerical models were obtained according to the procedures commented in the previous sections of this paper. As an example, the parameters used for the BVC24P60 model are shown in Tables 5, 6 and 7.

Table 5. Parameters for the model BVC24P60 – FEM.

Reinforced Concrete		Participating Masonry					
E_c (GPa)	í	E_x (MPa)	E_y (MPa)	í	ì	ó0 (MPa)	$f_{v,max}$ (MPa)
35	0.2	7560	10800	0.2	0.5	0.35	0.450

Table 6. Parameters for the model BVC24P60 – ESM.

Calculation method	E_d (MPa)	Strut width		Strut thickness		Eccentricities	
		w (cm)	w_{eff} (cm)	t (cm)	t_{ap} (cm)	e_H (cm)	e_L (cm)
Mainstone [23]	8469	67.82	-	19	-	54	46
Durrani and Luo [27]	8469	84.21	-	19	-	63	66
ABNT NBR 16868-1 [1]	8469	-	147.73	-	10	98	144

Table 7. Coefficient β for the model BVC24P60.

Calculation method	Number of struts	Position of strut	â
ABNT NBR 16868-1 [1]	1	Central	1.764
	2	Ends	1.487
	3	Central	1.477
	3	Ends	1.707

It is noteworthy that, for each of the twenty-four models, were simulated infilled frames applying the FEM (reference models), the classic ESM (single-strut), and also the two-strut and three-strut ESM (procedure proposed in section 3).

5 ANALYSES OF RESULTS

The lateral displacements of the infilled frame and the maximum shear force (V) in the column were analyzed. The lateral displacements were measured on the same point of the applied force F, while the maximum shear force was obtained in the contact region between the column and the infill masonry.

For the exhibiting of the results for each model, the following nomenclature was adopted:

- Expression from Maintone [23] – MA;
- Expression from Durrani and Luo [27] – DL;
- Expression from ABNT NBR 16868-1 [1] – NBR;
- Classic ESM (single-strut) – 1S;
- Two-strut ESM – 2S;
- Three-strut ESM – 3S.

Tables 8 and 9 show the results obtained. It was chosen the models with h_p equals to 60 cm (P60) to illustrate the order of magnitude of the values. It is noteworthy that, for the other models, the order of magnitude of the results were similar.

Table 8. Maximum shear force in the column (kN) for models P60.

Model	FEM	MA-1S	DL-1S	NBR-1S	MA-2S	DL-2S	NBR-2S	MA-3S	DL-3S	NBR-3S
BVC04P60	90.57	47.46	42.98	39.01	83.20	83.15	83.24	64.98	62.57	62.07
BVC14P60	196.95	56.48	48.60	38.82	172.59	172.53	172.99	112.69	108.26	103.94
BVC24P60	203.75	45.08	38.34	29.41	168.54	168.51	169.14	104.50	100.56	95.56
BCPV04P60	92.92	69.49	65.13	71.64	95.86	95.81	95.94	82.52	80.22	85.01
BCPM10P60	185.28	92.32	82.28	77.85	186.33	186.19	186.49	138.29	132.80	133.83
BCPM18P60	193.44	64.26	55.75	39.77	175.14	175.05	175.49	118.02	113.32	105.70

Table 9. Lateral displacements (mm) for models P60.

Model	FEM	MA-1S	DL-1S	NBR-1S	MA-2S	DL-2S	NBR-2S	MA-3S	DL-3S	NBR-3S
BVC04P60	1.83	2.03	1.84	1.67	2.26	2.15	2.31	2.06	1.88	1.86
BVC14P60	2.15	2.42	2.09	1.67	2.88	2.65	2.96	2.49	2.16	1.99
BVC24P60	1.82	1.93	1.65	1.27	2.36	2.16	2.44	2.00	1.72	1.54
BCPV04P60	2.67	2.96	2.78	3.05	3.19	3.08	3.51	3.00	2.82	3.21
BCPM10P60	3.29	3.94	3.52	3.33	4.49	4.09	4.81	4.03	3.61	3.76
BCPM18P60	2.40	2.75	2.39	1.71	3.24	2.99	3.02	2.83	2.47	2.04

To analyze the results, it was decided to normalize both the maximum shear force in the column and the lateral displacements. The normalization was performed through the ratio between the results obtained in the ESM models and the results obtained in reference models (FEM). The normalized results are displayed in sections 5.1 and 5.2 of this paper.

5.1 Maximum shear force in the column

The normalized maximum shear force in the column for each model are displayed in Figures 12 to 15, while the summary of the values grouped by ESM model are shown in Table 10.

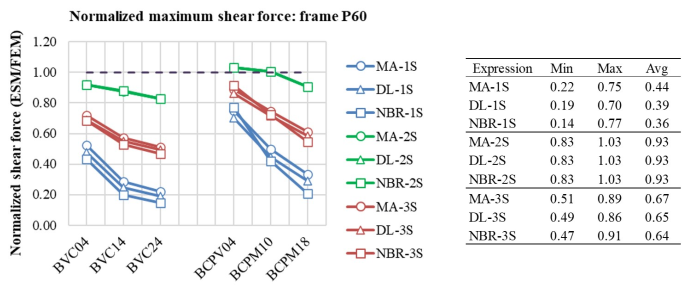

Figure 12. Normalized maximum shear force, frame P60.

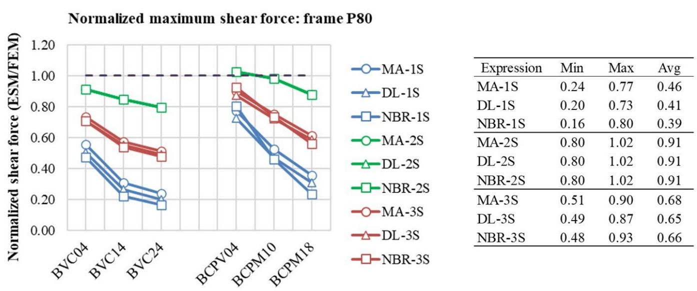

Figure 13. Normalized maximum shear force, frame P80.

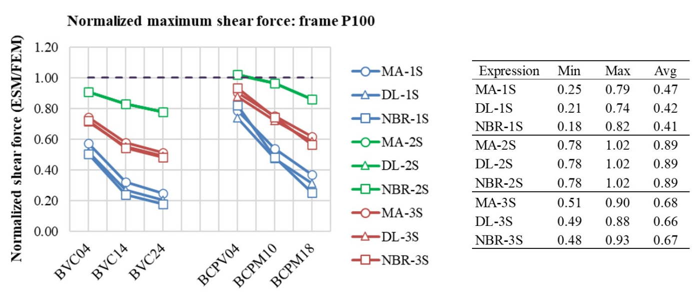

Figure 14. Normalized maximum shear force, frame P100.

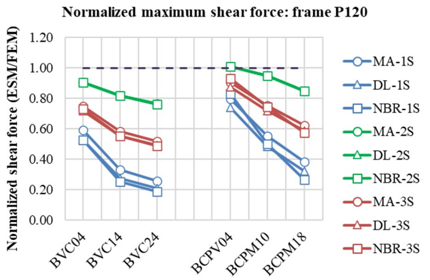

Expression	Min	Max	Avg
MA-1S	0.26	0.80	0.49
DL-1S	0.21	0.74	0.43
NBR-1S	0.19	0.83	0.43
MA-2S	0.76	1.01	0.88
DL-2S	0.76	1.01	0.88
NBR-2S	0.76	1.01	0.88
MA-3S	0.52	0.90	0.69
DL-3S	0.49	0.88	0.66
NBR-3S	0.49	0.93	0.67

Figure 15. Normalized maximum shear force, frame P120.

Table 10. Summary (grouped by ESM model) – normalized maximum shear force.

Model	Min	Max	Avg
1S	0.14	0.83	0.42
2S	0.76	1.03	0.90
3S	0.47	0.93	0.67

Based on the results obtained, it can be noted that the classic ESM (single-strut model) is inadequate to predict the maximum shear force in the column (in the region of contact with the infill masonry). On average, the shear force provided through the single-strut model represented only around 42% of the maximum shear force provided by the FEM results (Table 10). For masonry of higher stiffness, this discrepancy is even greater, with the single-strut model providing a maximum shear force that represents only 14% of the value provided by FEM, in the most against safety situation (BVC24P60V60, with the expression NBR-1S).

The two-strut model was the one that predicted, in a more satisfactory way, the maximum shear force in the column, providing, on average, values 10% lower than the maximum shear force from FEM models (Table 10). For frames infilled with masonry of higher modulus of elasticity, the two-strut model provided lower results relative to FEM, with a difference of up to 24% (BVC24P120V60); for frames infilled with masonry of lower modulus of elasticity, the results were closer to the reference, with two-strut models providing results up to 3% higher in relation to FEM (BCPV04P60V60). It should be noted that the expression used to calculate the properties of the equivalent strut practically does not change the value of the maximum shear force in the two-strut models, which is why in Figures 12 to 15 it is not possible to observe the results of the MA-2S and DL-2S, which are covered by the NBR-2S results.

The three-strut model provided better results than those of the classic single-strut model; however, it did not provide satisfactory results when compared to the two-strut model. The maximum shear force provided by the three-strut model were lower in relation to FEM in all cases analyzed (as well as the single-strut model) with differences around 33%, on average (Table 10). For frames infilled with masonry of higher modulus of elasticity, the difference was up to 53% (BVC24P60V60, with the expression NBR-3S), while for frames infilled with masonry of lower modulus of elasticity, it was up to 7% (BCPV04P60V60, with the NBR-3S expression). The two-strut and three-strut models (modeled according to the procedure proposed in this paper) provided less satisfactory results for masonry of high stiffness.

For the three-strut model, the expression from Mainstone [23] was the one that provided the most satisfactory results (taking as criterion an analysis in favor of safety and closest as possible to the FEM results), with values on average 32% lower than the maximum shear force provided by the reference models (Figures 12 to 15).

Thus, it was confirmed that the classic single-strut model underestimates the maximum shear force in the column (this model cannot describe properly the local effects resulting from the interaction between the infill wall and surrounding frame, as mentioned in section 2). On the other hand, the two-strut and three-strut models can predict additional shear forces in the column caused by the contact pressure between frame and wall, since these models possess struts that is not connected to the beam-column joints (eccentric struts).

Analyzing the results shown in Figures 12 to 15, it is clearly seen that, for both type of structural blocks (concrete and clay), the stiffer the masonry, more the results of the ESM models were against safety, i.e., lower than reference results (FEM models). Regarding the variation of the cross section of the columns, no significant differences were noted on the results.

5.2 Lateral displacement

The normalized lateral displacement for each model is displayed in Figures 16 to 19, while the summary of the values grouped by ESM model are shown in Table 11.

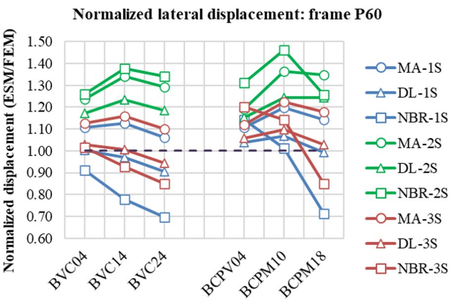

Expression	Min	Max	Avg
MA-1S	1.06	1.20	1.12
DL-1S	0.91	1.07	1.00
NBR-1S	0.70	1.14	0.87
MA-2S	1.19	1.36	1.30
DL-2S	1.15	1.24	1.21
NBR-2S	1.26	1.46	1.33
MA-3S	1.10	1.22	1.15
DL-3S	0.94	1.10	1.03
NBR-3S	0.85	1.20	1.00

Figure 16. Normalized lateral displacement, frame P60.

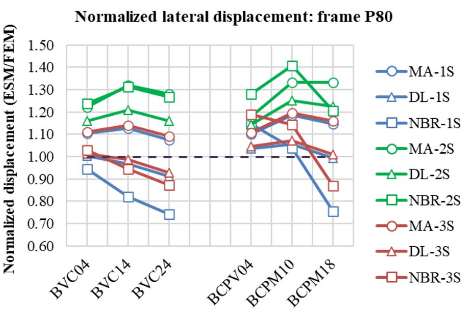

Expression	Min	Max	Avg
MA-1S	1.08	1.18	1.12
DL-1S	0.91	1.06	0.99
NBR-1S	0.74	1.15	0.91
MA-2S	1.18	1.33	1.28
DL-2S	1.14	1.25	1.19
NBR-2S	1.21	1.41	1.29
MA-3S	1.09	1.19	1.13
DL-3S	0.93	1.07	1.01
NBR-3S	0.87	1.19	1.01

Figure 17. Normalized lateral displacement, frame P80.

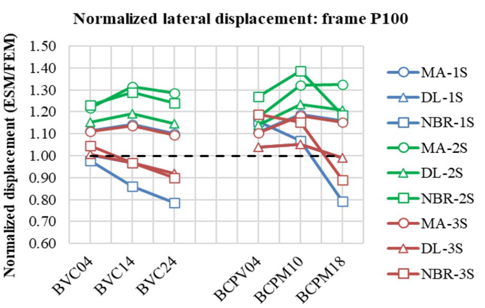

Expression	Min	Max	Avg
MA-1S	1.10	1.19	1.14
DL-1S	0.92	1.05	1.00
NBR-1S	0.79	1.16	0.94
MA-2S	1.17	1.32	1.27
DL-2S	1.14	1.23	1.18
NBR-2S	1.18	1.39	1.27
MA-3S	1.09	1.18	1.13
DL-3S	0.92	1.05	1.00
NBR-3S	0.89	1.19	1.02

Figure 18. Normalized lateral displacement, frame P100.

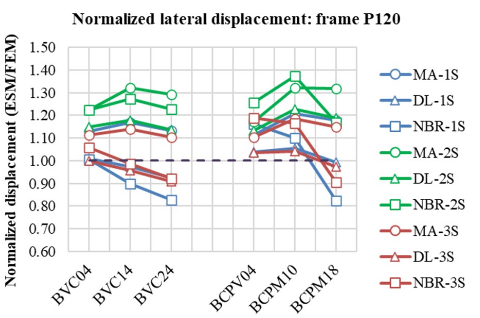

Expression	Min	Max	Avg
MA-1S	1.11	1.21	1.16
DL-1S	0.93	1.06	1.00
NBR-1S	0.83	1.16	0.97
MA-2S	1.17	1.32	1.28
DL-2S	1.13	1.23	1.17
NBR-2S	1.17	1.37	1.25
MA-3S	1.10	1.18	1.13
DL-3S	0.91	1.04	0.99
NBR-3S	0.91	1.19	1.04

Figure 19. Normalized lateral displacement, frame P120.

Table 11. Summary (grouped by ESM model) – normalized lateral displacement.

Model	Min	Max	Avg
1S	0.70	1.21	1.02
2S	1.13	1.46	1.25
3S	0.85	1.22	1.05

By analyzing the results obtained, the differences between the ESM and FEM (reference) models, on average, were: 2% for the single-strut model; 25% for the two-strut model; 5% for the three-strut model (Table 11). Thus, the classic single-strut model was the one that provided the closest displacements compared to the FEM (on average). However, single-strut model showed results up to 30% lower than the reference (BVC24P60V60, with the expression NBR-1S), while in the three-strut model, the biggest difference against safety was 15% (BVC24P60V60, with the expression NBR-3S).

The two-strut model provided the largest displacements. Its results were higher than the reference ones in all analyzed cases, with values up to 46% higher than those provided by the FEM (BCPM10P60V60, with the NBR-3S expression). The single-strut and three-strut models provided higher and lower results than the FEM. For the single-strut model: the maximum differences (higher in relation to FEM) and minimum (lower in relation to FEM) were 21% and 30%, respectively. Similarly, for the three-strut model, such differences were 22% and 15% (Table 11).

The expression from Durrani and Luo [27] was the one that provided the closest displacements in relation to FEM. In the three-strut model, the maximum difference (in favor of safety) and minimum (against safety) in relation to the FEM models were 10% (Figure 16) and 9% (Figure 19), respectively. In analogous comparison, for the three-strut model, the expression from Mainstone [23] provided results higher than FEM in all cases, with displacements 14% higher, on average; as for the ABNT NBR 16868-1 [1] expression, the differences in relation to the MEF were 20% (maximum) and 15% (minimum), both displayed at Figure 16.

The displacements provided by three-strut models were slightly larger in relation to the classic single-strut model, with difference of 3%, on average (Table 11). It is worth noting that, in the single-strut and three-strut models, the procedure of ABNT NBR 16868-1 [1] was the one that provided more less satisfactory results (against to safety), when compared to the reference displacements.

It can be concluded that, differently from observed about the maximum shear force in the column (section 5.1), the classic single-strut model can provide an adequate estimation of the lateral displacement of the infilled frame (although against safety in some situations). It indicates that this model can still be an adequate tool when the analysis is focused on the global response of the structure.

For the multi-strut models, it is important to highlight that the values of the eccentricities significantly influence the stiffness of the infilled frame. The application of the proposed procedures showed that the two-strut models are more flexible than the reference model (FEM). The three-strut models provided more reasonable results (displacements) than the classic ESM, when compared to reference models. Even though, the three-strut models provided results against safety for the maximum shear force in columns.

Regarding the variation in the cross section of the columns, no significant differences were noted in the results. In relation to the stiffness of the infill masonry, it is not possible to clearly see its influence from the results shown in Figures 16 to 19. However, it can be noticed that the increase in masonry stiffness provided lower displacements as compared to FEM in the single-strut and three-strut models with the expressions from Durrani and Luo [23] and from ABNT NBR 16868-1 [1].

6 CONCLUSIONS

In this study a procedure for equivalent multi-strut models were proposed, where the eccentricity of the equivalent struts is calculated as a function of the equivalent strut width, which can be obtained from any expression found in literature. For this purpose, three expressions were investigated: Mainstone [23], Durrani and Luo [27] and the ABNT NBR 16868-1 [1]. It is noteworthy that linear elastic analyzes were conducted and that the orthotropy of the infill masonry was considered. Based on the numerical simulations performed in this study, the following are highlighted as the main conclusions:

- The classic single-strut model is not appropriate to predict the maximum shear forces in the column, that occurs in the region of contact with the infill masonry, providing significantly lower values than those obtained with the FEM models (58% lower, on average); it is noteworthy that the difference is even more expressive when analyzing the frames infilled with masonry of higher modulus of elasticity, reaching up to 86% of difference (against safety). The two-strut model was able to satisfactorily predict the maximum shear force on the column, regardless of the expression used to determine the properties of the equivalent struts, with results about 10% lower than the reference ones. Although the three-strut model provided less satisfactory results than the two-strut one (33% lower in relation to FEM), it was better than the classic single-strut model for obtaining the maximum shear force in the column.

- Regarding lateral displacements, the three-strut model provided satisfactory results (5% higher in relation to FEM), with displacements slightly higher than those obtained in single-strut model. It was noted that the expression from ABNT NBR 16868-1 [1] applied to the three-strut model brings better results than when applied to the classic single-strut one. On the other hand, the two-strut model significantly overestimated the lateral displacements; in this model, the expression from Durrani and Luo [27] was the one that led to closer results in relation to FEM (19% higher displacements, on average). It is noteworthy that the expression from Mainstone [23], applied to the three-strut model, provided results in favor of safety in all analyzed cases, with displacements about 14% higher than the reference ones.
- Masonry stiffness influenced the results of the ESM models. Especially about the maximum shear force in the column, it was noted that the ESM models provided less satisfactory results for masonry of high stiffness, when compared to the FEM models. The stiffness of the column did not significantly influence the models analyzed in this study.
- Taking as a criterion an analysis in favor of safety and closest as possible to the FEM results, the expression from Mainstone [23] applied to the three-strut model is recommended to obtain the lateral displacement of the infilled frame; to obtain the maximum shear force in the column, the two-strut model is recommended, regardless of the expression used to determine the properties of the equivalent diagonals.

ACKNOWLEDGEMENTS

To National Council for Scientific and Technological Development – CNPq for financial support to the second author (Process: 308720/2018-0).

REFERENCES

[1] Associação Brasileira de Normas Técnicas, *Alvenaria Estrutural – Parte 1: Projeto*, NBR 16868-1, 2020.

[2] R. Alvarenga, “Análise teórico-experimental de estruturas compostas de pórticos de aço preenchidos com alvenaria de concreto celular autoclavado,” Ph.D. dissertation, Univ. São Paulo, São Carlos, 2002. [Online]. Available: https://www.teses.usp.br/teses/disponiveis/18/18134/tde-22032016-102411/pt-br.php

[3] E. Santos, “Influência da alvenaria no comportamento estrutural de edifícios altos de concreto armado,” M.S. thesis, Univ. Catol. Pernambuco, Recife, 2007. [Online]. Available: https://bdtd.ibict.br/vufind/Record/UCAP_1a457f6ecad042d1ffe0c54d696767d6

[4] L. Silva, “Modelagem de pórticos de concreto armado preenchidos com a consideração de aberturas nos painéis de alvenaria,” M.S. thesis, Univ. Fed. Santa Maria, Santa Maria, 2014. [Online]. Available: https://repositorio.ufsm.br/handle/1/7850

[5] P. Sousa, “Efeito dos painéis de vedação nas características dinâmicas de edificações de concreto armado,” M.S. thesis, Univ. Fed. Rio de Janeiro, Rio de Janeiro, 2014. [Online]. Available: http://www.coc.ufrj.br/pt/dissertacoes-de-mestrado/380-msc-pt-2014/4439-paulo-victor-almeida-de-sousa

[6] G. Alva, J. Kaminski Jr., G. Mohamad, and L. Silva, "Serviceability limit state related to excessive lateral deformations to account for infill walls in the structural model," *Ibracon Struct. Mater. J.*, vol. 8, no. 3, pp. 390–426, 2015. https://doi.org/10.1590/S1983-41952015000300008.

[7] M. Pitanga, “Contribuição ao estudo de pórticos de concreto armado preenchidos com alvenaria de blocos cerâmicos,” Ph.D. dissertation, Univ. Fed. Pernambuco, Recife, 2016. [Online]. Available: https://repositorio.ufpe.br/handle/123456789/25297

[8] G. Montandon, “Modelos estruturais para a análise de pórticos preenchidos com blocos cerâmicos em edifícios de concreto armado,” M.S. thesis, Univ. Fed. Uberlândia, Uberlândia, 2018. [Online]. Available: https://repositorio.ufu.br/handle/123456789/22409

[9] A. Grandi, “Avaliação experimental por meio de ensaios cíclicos de pórtico de aço preenchido com alvenaria participante,” M.S. thesis, Univ. Fed. Viçosa, Viçosa, 2018. [Online]. Available: https://www.locus.ufv.br/handle/123456789/20571

[10] W. Medeiros, “Pórticos em concreto pré-moldado preenchidos com alvenaria participante,” M.S. thesis, Univ. Fed. São Carlos, São Carlos, 2018. [Online]. Available: https://repositorio.ufscar.br/handle/ufscar/10029?show=full

[11] R. Santos, “Avaliação numérica de pórticos de aço preenchidos com painéis de alvenaria estrutural de blocos de concreto submetidos à carregamentos cíclicos,” M.S. thesis, Univ. Fed. Viçosa, Viçosa, 2019. [Online]. Available: https://www.locus.ufv.br/handle/123456789/26820

[12] L. Queiroz, “Alvenarias participantes: consideração e efeitos em edifícios de concreto sob ações horizontais,” M.S. thesis, Univ. Fed. Uberlândia, Uberlândia, 2020, http://dx.doi.org/10.14393/ufu.di.2020.377.

[13] A. Rigão, “Modelagem de pórticos em concreto armado preenchidos com alvenaria participante,” Ph.D. dissertation, Universidade Federal de Santa Maria, Santa Maria, 2022. [Online]. Available: https://repositorio.ufsm.br/handle/1/24212

[14] L. Galvão, “Contribuições à análise numérica de edifícios com alvenarias paricipantes,” M.S. thesis, Universidade Federal de Uberlândia, Uberlândia, 2022. [Online]. Available: https://repositorio.ufu.br/handle/123456789/34463

[15] S. Polyakov, *On the Interaction Between Masonry Filler Walls and Enclosing Frame When Loaded in the Plane of the Wall*. São Francisco, CA: Earthquake Engineering Research Institute, 1960, pp. 36–42.

[16] M. Holmes, "Steel frames with brickwork and concrete infilling," *Proc.- Inst. Civ. Eng.*, vol. 19, no. 4, pp. 473–478, 1961, http://dx.doi.org/10.1680/iicep.1961.11305.

[17] B. Stafford-Smith, "Lateral stiffness of infilled frames," *J. Struct. Div.*, vol. 88, no. 6, pp. 183–199, 1962., http://dx.doi.org/10.1061/JSDEAG.0000849.

[18] B. Stafford-Smith, "Behaviour of square infilled frames," *J. Struct. Div.*, vol. 92, no. 1, pp. 381–403, 1966., http://dx.doi.org/10.1061/JSDEAG.0001387.

[19] B. Stafford-Smith, "The composite behaviour of infilled frames," in *Tall Buildings*, A. Coull and B. Stafford-Smith, Ed., London: Pergamon Press, 1967, pp. 481–495.

[20] B. Stafford-Smith, "Methods of predicting the lateral stiffness and strenght of multi-storey infilled frames," *Build. Sci.*, vol. 2, no. 3, pp. 247–257, 1967., http://dx.doi.org/10.1016/0007-3628(67)90027-8.

[21] B. Stafford-Smith and C. Carter, "A method of analysis for infilled frames," *Proc.- Inst. Civ. Eng.*, vol. 44, no. 1, pp. 31–48, 1969., http://dx.doi.org/10.1680/iicep.1969.7290.

[22] A. Hendry, *Structural Brickwork.* London: MacMillan, 1981.

[23] R. Mainstone, *Supplementary Note on the Stiffness and Strengths of Infilled Frames*. Garston, UK: Building Research Station, 1974.

[24] T. Liauw and K. Kwan, "Nonlinear behavior of non-integral infilled frames," *Comput. Struc.*, vol. 18, no. 3, pp. 551–560, 1984., http://dx.doi.org/10.1016/0045-7949(84)90070-1.

[25] L. Decanini and G. Fantin, "Modelos simplificados de la mampostería incluida en porticos: caracteristicas de rigidez y resistencia lateral en estado limite," *J. Argentinas de Ing. Estruct.*, vol. 2, pp. 817–836, 1987.

[26] T. Paulay and M. Priestley, *Seismic Design of Reinforced Concrete and Masonry Buildings*. New York: Wiley, 1992, http://dx.doi.org/10.1002/9780470172841.

[27] A. Durrani and Y. Luo, "Seismic retrofit of flat-slab buildings with masonry infills," in *Proc. NCEER Workshop on Seismic Response of Masonry Infills*, Buffalo, NY, 1994, pp. 1–8.

[28] C. Chrysostomou and P. Asteris, "On the in-plane properties and capacities of infilled frames," *Eng. Struct.*, vol. 41, pp. 385–402, 2012., http://dx.doi.org/10.1016/j.engstruct.2012.03.057.

[29] Applied Technology Council, *Evaluation of Earthquake Damaged Concrete and Masonry Wall Buildings, FEMA 306*, 1998.

[30] Masonry Standards Joint Committee, *Building Code Requirements for Masonry Structures*, TMS 402-16, 2016.

[31] Canadian Standards Association, *Design of Masonry Structures*, S304-14, 2014.

[32] New Zealand Standard, *Design of Reinforced Concrete Masonry Structures*, NZS 4230, 2004.

[33] W. El-Dakhakhni, M. Elgaaly, and A. Hamid, "Three-strut model for concrete mansory-infilled steel frames," *J. Struct. Eng.*, vol. 129, no. 2, pp. 177–185, 2003., http://dx.doi.org/10.1061/(ASCE)0733-9445(2003)129:2(177).

[34] F. Crisafulli and A. Carr, "Proposed macro-model for the analysis of infilled frame structures," *Bull. N. Z. Soc. Earthq. Eng.*, vol. 40, no. 2, pp. 69–77, 2007., http://dx.doi.org/10.5459/bnzsee.40.2.69-77.

[35] M. Yekrangnia and M. Mohammadi, "A new strut model for solid masonry infills in steel frames," *Eng. Struct.*, vol. 135, pp. 222–235, 2017., http://dx.doi.org/10.1016/j.engstruct.2016.10.048.

[36] S. Di Nino, "Numerical investigations on infilled frames and predictive formulae in the elastic regime," *Eng. Struct.*, vol. 250, no. 113349, pp. 113349, 2022., http://dx.doi.org/10.1016/j.engstruct.2021.113349.

[37] P. Lourenço, "Computacional strategies for masonry structures," Ph.D. dissertation, Delft Univ. Technol., Delft, 1996. [Online]. Available: https://repository.tudelft.nl/islandora/object/uuid%3A4f5a2c6c-d5b7-4043-9d06-8c0b7b9f1f6f

[38] G. Silva, "Escolha de parâmetros para análise de contato entre corpos elásticos usando elementos finitos e redes neurais," M.S. thesis, Univ. Est. Campinas, Campinas, 2009. [Online]. Available: https://www.repositorio.unicamp.br/handle/REPOSIP/265005

[39] T. Van and T. Lau, "Experimental evaluation of reinforced concrete frames with unreinforced masonry infills under monotonic and cyclic loadings," *Int. J. Civ. Eng.*, vol. 19, no. 4, pp. 401–419, 2021., http://dx.doi.org/10.1007/s40999-020-00576-7.

[40] I. Doudoumis, "Finite element modelling and investigation of the behaviour of elastic infilled frame under monotonic loading," *Eng. Struct.*, vol. 29, no. 6, pp. 1004–1024, 2007., http://dx.doi.org/10.1016/j.engstruct.2006.07.011.

[41] L. Cavaleri, M. Papia, G. Macaluso, F. Di Trapani, and P. Colajanni, "Definition of diagonal Poisson's ratio and elastic modulus foi infill masonry walls," *Mater. Struct.*, vol. 47, no. 1-2, pp. 239–262, 2014., http://dx.doi.org/10.1617/s11527-013-0058-9.

[42] L. Liberatore and L. Decanini, "Effect of infills on the seismic response of high-rise RC buildings designed as bare according to Eurocode 8," *Ing. Sism.*, vol. 28, no. 3, pp. 7–23, 2011.

[43] N. Noh, L. Liberatore, F. Mollaioli, and S. Tesfamariam, "Modelling of masonry infilled RC frames subjected to cyclic loads: State of the art review and modelling with OpenSees," *Eng. Struct.*, vol. 150, pp. 599–621, 2017., http://dx.doi.org/10.1016/j.engstruct.2017.07.002.

Author contributions: LFG: investigation, methodology, writing. GMSA: conceptualization, data curation, formal analysis, methodology, validation, writing.

Editors: Vladimir Haach, Guilherme Aris Parsekian.